

Original Article

Improvement of Electron Probe Microanalysis of Boron Concentration in Silicate Glasses

Lining Cheng^{1,2}, Chao Zhang^{2,3*}, Xiaoyan Li^{2,3}, Renat R. Almeev², Xiaosong Yang¹ and Francois Holtz²

¹State Key Laboratory of Earthquake Dynamics, Institute of Geology, China Earthquake Administration, 100029 Beijing, China; ²Institute of Mineralogy, Leibniz University Hannover, Callinstr. 3, 30167 Hannover, Germany and ³State Key Laboratory of Continental Dynamics, Department of Geology, Northwest University, 710069 Xi'an, China

Abstract

The determination of low boron concentrations in silicate glasses by electron probe microanalysis (EPMA) remains a significant challenge. The internal interferences from the diffraction crystal, i.e. the Mo-B₄C large *d*-spacing layered synthetic microstructure crystal, can be thoroughly diminished by using an optimized differential mode of pulse height analysis (PHA). Although potential high-order spectral interferences from Ca, Fe, and Mn on the BK α peak can be significantly reduced by using an optimized differential mode of PHA, a quantitative calibration of the interferences is required to obtain accurate boron concentrations in silicate glasses that contain these elements. Furthermore, the first-order spectral interference from CL-lines is so strong that they hinder reliable EPMA of boron concentrations in Cl-bearing silicate glasses. Our tests also indicate that, due to the strongly curved background shape on the high-energy side of BK α , an exponential regression is better than linear regression for estimating the on-peak background intensity based on measured off-peak background intensities. We propose that an optimal analytical setting for low boron concentrations in silicate glasses (≥ 0.2 wt% B₂O₃) would best involve a proper boron-rich glass standard, a low accelerating voltage, a high beam current, a large beam size, and a differential mode of PHA.

Key words: boron, electron probe microanalysis, high-energy background, silicate glass, tourmaline

(Received 23 December 2018; revised 29 April 2019; accepted 24 May 2019)

Introduction

Boron is generally present at trace level concentrations in natural extrusive or intrusive magmatic rocks, but its abundance can be significantly enriched in highly evolved silicic magmas (e.g., pegmatitic magmas). Boron usually behaves as an incompatible element in magmatic systems and its concentration increases in residual melts in the course of crystallization (London et al., 1996). Boron also has a high tendency to be partitioned into vapor during magmatic evolution (Pichavant, 1981), which prevents the accurate assessment of boron concentration in a magmatic system based only on bulk rock composition. It has been observed, in numerous experimental studies, that the presence of boron in granitic and pegmatic systems may have broad effects on modifying the physicochemical properties of silicate melts, such as melt viscosity, liquidus temperature, phase stability, water solubility, and water speciation (e.g., London, 1987; Holtz et al., 1993; Dingwell et al., 1996; London et al., 1996; Schmidt, 2004). In such experimental studies, boron concentrations have been commonly acquired by electron probe microanalysis (EPMA; McGee & Anovitz, 1996), by secondary ion mass spectrometry (SIMS) or by laser ablation-inductively coupled plasma mass

spectrometry (LA-ICPMS). Although it is clear that SIMS and LA-ICPMS have much lower detection limits for measuring boron concentrations (e.g., Jochum et al., 2000; Tiepolo et al., 2005), EPMA is still useful and capable of measuring boron contents in minerals and silicate glasses in many cases (see details below). Considering the ready access of EPMA, its high spatial resolution and non-destructive nature, it is valuable to improve the analytical capability of EPMA for low concentrations of boron in geological samples, particularly for silicate glasses formed in experimental studies that are focused on boron.

McGee & Anovitz (1996) provided a review on the progresses of EPMA of high boron contents (usually B₂O₃ > 10 wt%) in boron-rich minerals (e.g., tourmaline), which emphasized the great advance in the 1990s in detecting light elements by using large *d*-spacing layered synthetic microstructure (LSM) crystals (see also McGee et al., 1991). LSM crystals are also termed as layered dispersion elements (LDE) crystals by JEOL, or pseudo-crystals (PC) by CAMECA. Currently, the LSM crystal usually applied for detecting a boron K α spectrum is a Mo-B₄C multilayer-crystal with a *2d* value of 200 Å, which is termed as LDE3 by JEOL or PC3 by CAMECA. However, as noted by Kobayashi et al. (1995), McGee & Anovitz (1996) and Morgan (2015), using a Mo-B₄C LSM crystal as diffraction crystal may produce internal fluorescence from the boron atoms which would result in a false boron signal in the analyzed materials. It is also possible to detect a boron K α spectrum using the Ni-C-multilayer-crystal (*2d* = 100 Å, termed as LDE2 by JEOL

*Author for correspondence: Chao Zhang, E-mail: c.zhang@mineralogie.uni-hannover.de

Cite this article: Cheng L, Zhang C, Li X, Almeev RR, Yang X, Holtz F (2019) Improvement of Electron Probe Microanalysis of Boron Concentration in Silicate Glasses. *Microsc Microanal* 25, 874–882. doi:10.1017/S1431927619014612

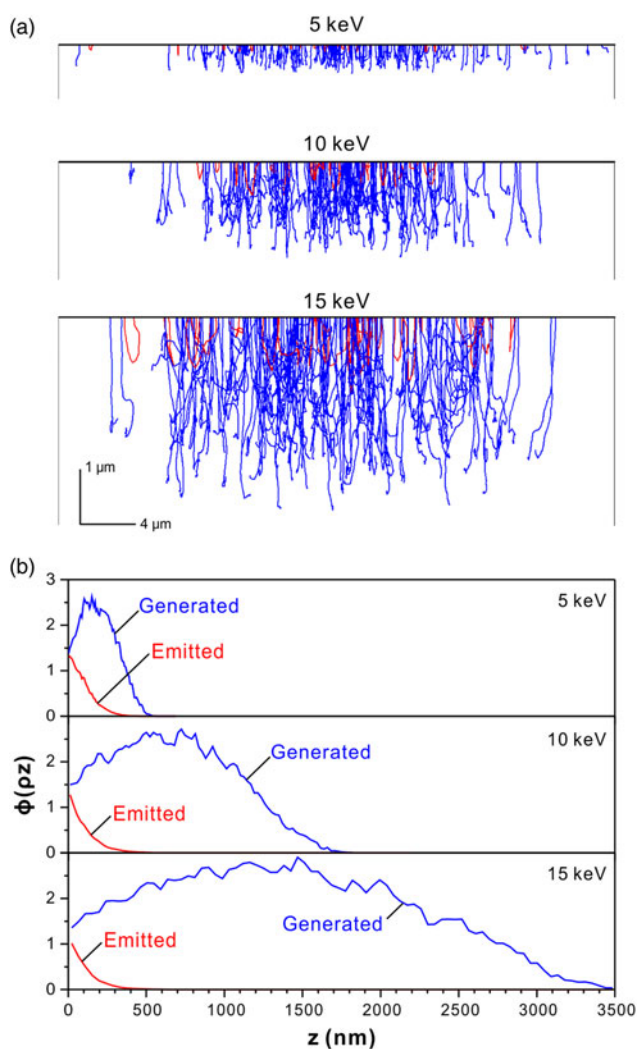


Fig. 1. Monte Carlo simulation displaying the effect of electron beam trajectory for EPMA of $BK\alpha$. **a:** The distribution of generated (blue) and emitted (red) characteristic X-rays. **b:** $\phi(\rho z)$ distributions of generated and emitted X-rays with depth. Simulation was performed using WinXRay program (Demers et al., 2002), with varied accelerating voltages, fixed beam current of 100 nA and beam diameter of 20 μm .

or PC2 by CAMECA); however, it yields much lower intensity and thus higher uncertainty than using PC3, although the false boron signal is absent (Fialin et al., 1996). In addition, the influence from the sharply curved high-energy background results in challenges in accurate quantification of the true on-peak background intensity from measurable off-peak background intensities (Morgan, 2015). McGee & Anovitz (1996) also noted that the boron peak intensity and peak/background ratio is enhanced if a lower accelerating voltage is used, probably due to reduced volume of excitation and thus depressed X-ray absorption. Indeed, as demonstrated by the results of Monte Carlo simulation performed using the WinX-ray program (Demers et al., 2002), the effective volume of fluorescence excitation is greatly enlarged at 15 keV compared to 5 keV (Fig. 1a); however, the emitted energy of characteristic X-rays of $BK\alpha$ is even depressed while the generated X-ray is enormously increased (Fig. 1b), indicating the strongly enhanced absorption with a high accelerating voltage.

Recently, Morgan (2015) noted the difficulties in using boron metal or boride compounds as standards for analyzing boron

contents in silicate and borate samples, because these materials have significant differences in X-ray absorption, background characteristics, and peak position and shape. However, neither the technical challenges mentioned by McGee & Anovitz (1996) and Morgan (2015), nor their useful hints have been discussed practically in literature. In this study, we carefully addressed the technical issues mentioned previously and tested some protocols for improving the analytical capability of EPMA for measuring low boron concentrations in silicate glasses.

Samples

One natural dravite tourmaline and several synthetic boron-bearing silicate glasses have been used in this study, and their compositions are listed in Table 1. The boron content of the natural dravite (Harvard 108796) was measured by various techniques including EPMA, SIMS, proton-induced gamma-ray emission (PIGE), and prompt gamma-ray neutron activation analysis (PGNAA) (Dyar et al., 2001), which yield a mean value of B_2O_3 content of 10.36 wt%.

One dry sodium borosilicate glass, NBS1-0, synthesized by Bauer et al. (2017), was used as a standard for measuring the boron content in silicate glasses in this study. The glass NBS1-0 contains 11.32 wt% B_2O_3 , which was measured by Bauer et al. (2017) using inductively coupled plasma-optic emission spectroscopy (ICP-OES). We also used a hydrous sodium borosilicate glass, NBS1-I, which was synthesized at 500 MPa and 1,150°C using the glass NBS1-0 as starting glass and deionized water (Bauer et al., 2017). Water content of the glass NBS1-I was determined as 0.91 wt% using Karl-Fischer titration, and therefore its B_2O_3 content can be calculated as 11.22 wt% from the composition of the starting glass NBS1-0.

Four boron-bearing dry rhyolitic glasses (B1, B4, B6, and B10) were synthesized at the Institute of Mineralogy, Leibniz University Hannover, from mixed powders of a nominally boron-free glass and H_3BO_3 , which were melted in a platinum crucible at 1,600°C for 2 h and then quenched to form glass. The nominally boron-free glass (BFG-1) was produced by melting the powder of a natural tourmaline-free granite (T10-65). The resulting boron-bearing glasses were then milled into fine-grained powder, remelted and quenched, and this process was repeated another two times in order to achieve glass homogenization. The amount of initial H_3BO_3 mixed to form the synthetic glasses were assigned to generated target B_2O_3 contents of 1, 4, 6, and 10 wt% in the glasses B1, B4, B6, and B10, respectively (Table 1). As indicated by the analytical results (see below), however, the final B_2O_3 contents in the synthesized glasses may be lower due to loss of boron during glass synthesis (Wenzel & Sanders, 1982; Holtz et al., 1993).

We also tested our analytical protocol on one boron-rich hydrous experimental glass, synthesized at the Institute of Mineralogy, Leibniz University Hannover in a crystallization experiment using the B10 glass as starting glass, mixed with 8 wt% H_2O at 300 MPa and 750°C for 480 h in a cold sealed press vessel (CSPV). The products of this experiment include glass (DC-10, Table 1) and tourmaline. EPMA on scattered spots of the experimental glass showed no compositional heterogeneity. Another three low-boron hydrous rhyolitic glasses (B0.5, B0.2, and B0.1) were synthesized by mixing the boron-free glass (BFG-1) and the B1 glass and subsequent melting. For each synthesis procedure, the mixed glass powders, together with 4 wt% deionized water added into the mixture, were sealed in a gold

Table 1. Compositions of Boron-Bearing Materials Used in This Study (wt%).

Sample	SiO ₂	TiO ₂	Al ₂ O ₃	FeO _T ^a	MnO	MgO	CaO	Na ₂ O	K ₂ O	B ₂ O ₃ ^b	Cl	H ₂ O	Total	B ₂ O ₃ (LA-ICPMS) ^c			B ₂ O ₃ (EPMA, 15 keV)			B ₂ O ₃ (EPMA, 10 keV)			B ₂ O ₃ (EPMA, 5 keV)		
														<i>n</i>	wt%	σ	<i>n</i>	wt%	σ	<i>n</i>	wt%	σ	<i>n</i>	wt%	σ
Dravite ^d	35.28	1.63	22.31	13.99	0.02	8.66	2.54	1.49	0.06	10.36 ^e	n.d.	2.30 ^e	98.64	n.d.	n.d.	n.d.	n.a.	n.d.	n.d.	n.a.	n.d.	n.d.	n.a.	n.d.	n.d.
NBS1-0 ^f	72.51	0.00	0.00	0.00	0.00	0.00	0.00	0.00	0.00	11.32	0.00	0.00	100.00	n.d.	n.d.	n.d.	n.a.	n.d.	n.d.	n.a.	n.d.	n.d.	n.a.	n.d.	n.d.
NBS1-I ^f	71.82	0.00	0.00	0.00	0.00	0.00	0.00	16.03	0.00	11.22	0.00	0.91	99.98	n.d.	n.d.	n.d.	10	11.05	0.42	10	11.32	0.23	10	11.40	0.20
RHY-G ^g	74.46	0.02	14.03	1.02	0.00	0.00	0.39	4.68	5.26	0.00	b.d.l.	0.00	99.86	5	b.d.l.	n.d.	10	0.38	0.21	10	0.25	0.09	10	0.21	0.06
BFG-1	73.39	0.14	15.03	1.18	0.03	0.27	0.87	3.66	4.49	0.00	b.d.l.	0.00	99.06	5	n.d.	n.d.	10	b.d.l.	n.d.	10	b.d.l.	n.d.	10	b.d.l.	n.d.
DC-10	72.82	0.20	15.26	1.21	0.02	0.23	1.01	3.70	4.44	n.d.	b.d.l.	n.d.	94.36	5	n.d.	n.d.	10	7.68 ^h	0.28	10	7.60 ^h	0.18	10	7.85 ^h	0.24
B10	66.51	0.13	13.25	1.12	0.03	0.19	0.80	3.36	3.63	10.00	b.d.l.	0.00	99.00	5	8.54	0.03	10	8.52 ^h	0.34	10	8.26 ^h	0.22	10	8.64 ^h	0.20
B6	69.52	0.13	13.87	1.06	0.03	0.13	0.80	3.55	3.88	6.00	b.d.l.	0.00	98.98	5	5.37	0.02	10	5.26 ^h	0.30	10	5.30 ^h	0.20	10	5.56 ^h	0.18
B4	70.34	0.14	14.33	1.21	0.04	0.19	0.93	3.42	4.08	4.00	b.d.l.	0.00	98.67	5	3.74	0.02	10	3.68 ^h	0.20	10	3.72 ^h	0.16	10	3.80 ^h	0.25
B1	72.01	0.15	14.73	1.22	0.03	0.19	0.96	3.56	4.33	1.00	b.d.l.	0.00	98.19	5	0.94	0.01	10	0.81 ^h	0.12	10	1.02 ^h	0.15	10	0.99 ^h	0.14
B0.5	69.52	0.17	14.40	1.16	0.03	0.20	0.95	3.48	4.21	0.52	b.d.l.	4.00 ⁱ	98.64	5	0.50	0.01	10	b.d.l.	n.d.	10	0.45 ^h	0.12	10	0.48 ^h	0.12
B0.2	69.75	0.18	14.55	1.16	0.02	0.22	0.96	3.53	4.24	0.21	b.d.l.	4.00 ⁱ	98.82	5	0.20	0.01	10	b.d.l.	n.d.	10	b.d.l.	n.d.	10	0.18 ^h	0.08
Detection limit	-	-	-	-	-	-	-	-	-	-	0.02	-	-	-	-	-	-	0.63	-	-	0.27	-	-	0.18	-

n, analytical number; σ, standard deviation; b.d.l., below detection limit; n.d., not determined.

^aTotal iron content is expressed as FeO.

^bB₂O₃ contents from literature (for dravite, NBS1-0, and NBS1-I) or nominal B₂O₃ contents in the starting materials prepared for glass synthesis.

^cB₂O₃ contents were measured by LA-ICPMS using NIST610 (containing 350 ppm boron, ref. Jochum et al., 2011) as calibration reference and SiO₂ content measured by EPMA as internal calibration standard. Detection limit of LA-ICPMS for boron is ~1.5 ppm.

^dDravite reference from Dyar et al. (2001).

^eMean value of results from four different analytical methods (Dyar et al., 2001).

^fSynthetic borosilicate glasses from Bauer et al. (2017).

^gSynthetic boron-free rhyolitic glass from Zhang et al. (2016).

^hB₂O₃ contents measured by EPMA have been corrected via subtracting the background-induced apparent B₂O₃ content of boron-free glass RHY-G.

ⁱContent of added H₂O for glass synthesis.

Other notes: Except for boron, other elements of B-bearing silicate glasses were analyzed using an accelerating voltage of 15 keV, a beam current of 5 nA and a beam size of 20 μm. B₂O₃ contents analyzed using three different accelerating voltage (15 keV, 10 keV and 5 keV), but with a same beam current (100 nA) and beam size (20 μm), are listed individually. B₂O₃ contents have been calibrated for the potential interferences from Ca, Fe, and Mn based on measurements of interference-induced fake boron intensity in plagioclase (An95), olivine (Fo83) and Mn₃O₄, assuming a linear effect of the calibration. Peak time for calibration and subsequent analyses was always set as 60 s.

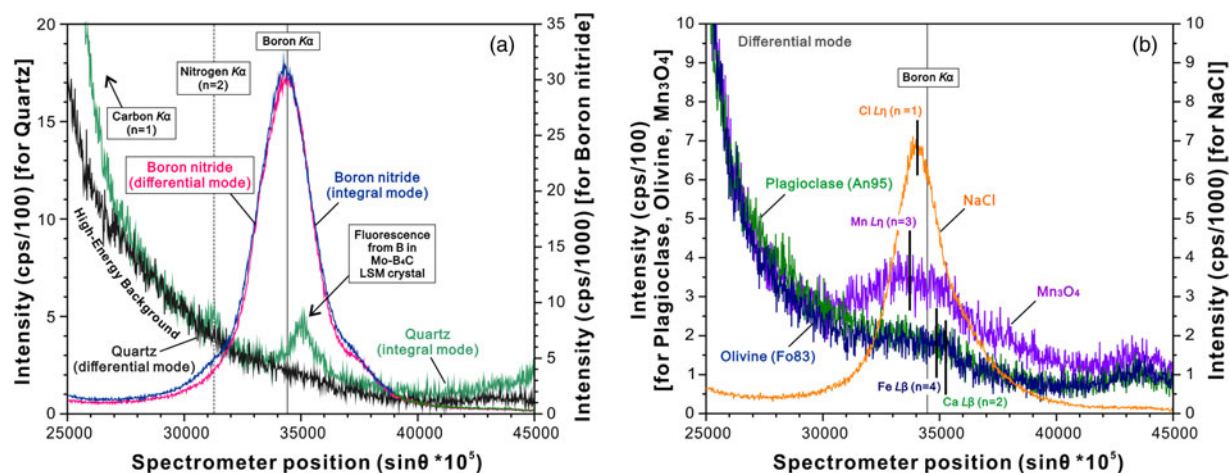


Fig. 2. Spectral scans of several reference materials at the adjacent of $BK\alpha$ peak acquired with PC3 diffraction crystal ($2d = 200 \text{ \AA}$) on CAMECASX-100 microprobe. **a:** Spectral scans of quartz and boron nitride. Using a differential mode instead of an integral mode can diminish the internal fluorescence from the Mo- B_4C crystal. Note that the extremely high peak signal of boron nitride is contributed from both boron and nitrogen. **b:** Spectral scans of plagioclase (An95, CaO 19.09 wt%), olivine (Fo83, FeO 16.62 wt%), Mn_3O_4 and NaCl. Differential mode: baseline = 1,400 mV, window = 4,200 mV. Accelerating voltage = 15 keV; beam current = 100 nA; dwell time = 100 ms; accumulation number = 3.

capsule and then placed in internally heated pressure vessel (IHPV) at 200 MPa and 1,000°C for 50 h. To complete melting, the capsules were dropped down to a cold zone ($\sim 50^\circ\text{C}$) with an estimated quench rate of $\sim 150^\circ\text{C/s}$ (Berndt et al., 2002). The synthesized glasses were checked with optical microscope and electron microprobe back-scattered electron images, and no crystalline phases were observed. According to the relative masses in the starting materials weighed prior to mixing prepared for glass synthesis, the calculated nominal B_2O_3 contents of the resultant low-boron glasses B0.5, B0.2, and B0.1 are 0.52, 0.21, and 0.11 wt%, respectively (Table 1).

Analytical Settings

EPMA

The analyses in this study were performed with a CAMECA SX-100 microprobe equipped with five spectrometers and the PeakSight operating system, at the Institute of Mineralogy, Leibniz University Hannover. A PC3 crystal (i.e., LSM crystal made of Mo- B_4C , $2d = 200 \text{ \AA}$) was used for detecting boron. For each analysis, major elements other than boron were first measured with an accelerating voltage of 15 keV, a beam current of 5 nA and a beam size of $20 \mu\text{m}$ with a total acquisition time of 40 s. Boron was measured subsequently with a second condition. For achieving an optimal setting for analyzing B concentration in silicate glasses, we tested several approaches for increasing B signal intensity and better quantifying background, which included quantification of background from B-free materials, modifications in parameters for the pulse height analysis (PHA), accelerating voltage, and beam current.

LA-ICPMS

In order to clarify the accuracy of EPMA protocol established in this study, boron concentrations of some synthetic glasses were also measured by LA-ICPMS at the Institute of Mineralogy, Leibniz University Hannover. The laser ablation system was in-house built, based on a Spectra-Physics Solstice femtosecond

laser operating in the deep UV at 194 nm, and the regenerative amplified system was pumped at 500 Hz, generating a pulse energy of 70 mJ at this wavelength. The elemental analyses were conducted using an Element XR fast scanning sector field ICP-MS (ThermoScientific). The detailed description of operation conditions and procedures can be found in Horn et al. (2006) and Zhang et al. (2017). The SiO_2 content determined by EPMA was used as internal standard (^{29}Si), and the quantification of the boron concentration was performed based on the NIST SRM 610 reference glass (~ 350 ppm boron; ref. Jochum et al., 2011). Data processing was performed using the SILLS software package (Guillong et al., 2008).

Results

Testing Result for PHA

As shown in Figure 2a, the spectrum of quartz acquired using an integral mode at the adjacent range of the $BK\alpha$ peak involves contributions of the fluorescences from B and Mo in the PC3 crystal, in agreement with the observations of McGee & Anovitz (1996) and Morgan (2015). It is shown here that these fluorescence-induced inferences can be eliminated by using differential mode with a PHA that filters the received X-ray by height (i.e., energy). Therefore, all the following tests and analyses have been performed with a differential mode, and optimal setting of the PHA with a baseline of 1,400 mV and window of 4,200 mV can eliminate thoroughly the fluorescence-induced inferences and meanwhile obtain a strong signal of $BK\alpha$. The spectra of quartz at this acquisition condition also demonstrates that the potential high-order $OK\alpha$ has been diminished. In addition, boron nitride has a very strong but broad apparent peak around $BK\alpha$, which likely arises from overlapped $K\alpha$ peaks of boron and nitrogen because 2λ of $NK\alpha$ is very close to 1λ of $BK\alpha$, and thus boron nitride is unsuitable as standard for analyzing boron-bearing silicate minerals or glasses. The spectrum of plagioclase (An95), olivine (Fo83), and Mn_3O_4 shown in Figure 2b indicate that, in spite of using an optimized differential mode, there are still slight high-order spectral interferences from Ca, Fe, and Mn at the peak

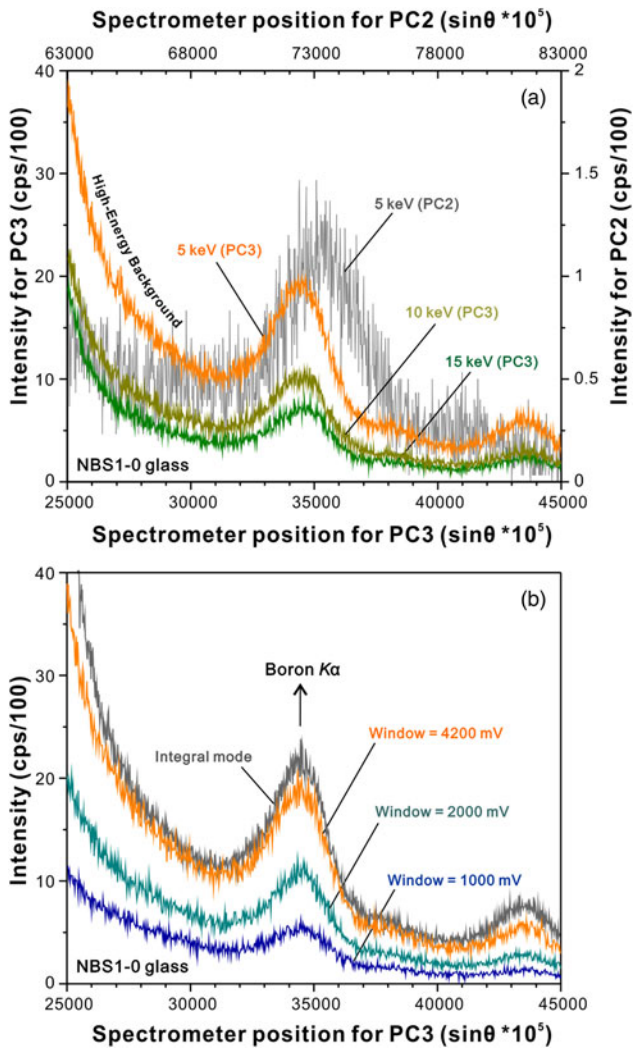


Fig. 3. Optimization of voltage and PHA for detecting $BK\alpha$. **a:** Effect of diffraction crystal (PC2 and PC3) and accelerating voltage on intensity of $BK\alpha$ signal. Beam current = 100 nA; dwell time = 0.1 s; accumulation number = 3. **b:** Effect of PHA window (using PC3 as diffraction crystal) on $BK\alpha$ signal. The tests were made on the reference glass NBS1-0 ($B_2O_3 = 11.32$ wt%). Accelerating voltage = 5 keV; beam current = 100 nA; dwell time = 100 ms; accumulation number = 3.

of $BK\alpha$ (McGee *et al.*, 1991), which are significant and should be allowed for when obtaining accurate low concentrations of boron in silicate glasses that contain Ca, Fe, and Mn as major elements (Table 1). On the other hand, Cl shows a strong first-order L -line peak near the $BK\alpha$ peak, which results in enormous interference that is not relievable by using an optimized differential mode (McGee *et al.*, 1991). However, Cl is lacking in the materials used in this study, and therefore the potential interference from Cl will not be addressed further. Fortunately, the glass NBS1-0 contains no Ca, Fe, Mn or Cl, which enables it as an ideal standard material for EPMA of boron.

Testing Result for Accelerating Voltage

We tested the effect of lowering accelerating voltage on increasing $BK\alpha$ intensity (McGee & Anovitz, 1996). As shown in Figure 3a, the spectral intensity of glass NBS1-0 acquired with a voltage of 5 keV is significantly higher than that acquired with a voltage of 15 keV. Both peak intensity and the surrounding background

intensity are enhanced, which roughly results in a doubled net intensity (peak-background) for detecting $BK\alpha$. Therefore, for analyzing low B_2O_3 contents in silicate glasses (<1 wt%), we suggest using a voltage of 5 keV; however, for silicate glasses with a B_2O_3 content higher than 1 wt%, a voltage of 10 or 15 keV is recommended, which would facilitate simultaneous measurements of other heavier elements. In order to reduce the sharply increasing background on the high-energy side of $BK\alpha$ that is likely due to carbon $K\alpha$, we tested two modified differential modes with narrowed windows of PHA. The results in Figure 3b indicate that the high-energy side background of $BK\alpha$ can be significantly reduced by using a narrower window of PHA (2,000 and 1,000 mV versus 4,200 mV), but the peak intensity of $BK\alpha$ is also strongly reduced. Therefore, we do not recommend using a narrow window of PHA for detecting $BK\alpha$, and we kept using a window of 4,200 mV in the following analyses.

Testing Result for Reference Materials

An ideal primary standard of EPMA for boron should be well-characterized, homogeneous materials with similar compositions to unknown samples, and having a high content of boron (McGee & Anovitz, 1996). Tourmaline and rhyolitic glass are two of the most commonly encountered materials for boron content analysis. In this study, we compare the $BK\alpha$ signals and background shapes of the dravite tourmaline (Harvard 108796) and borosilicate glass NBS1-0, which have very similar B_2O_3 contents, i.e., 10.36 and 11.32 wt%, respectively. As shown in Figure 4a, the spectral shapes of the dravite and the glasses NBS1-0 and B10 are very similar, but the dravite has apparently lower background than the glasses at the high-energy side. This difference is likely due to varied X-ray absorption in the mineral and silicate glass. As a result, if both sides of background are considered in data acquisition and processing for the determination of boron content, the dravite (10.36 wt% B_2O_3) would clearly yield a higher calibration intensity (i.e., count rate of net peak signal per unit of boron content) than the glass NBS1-0 (11.32 wt% B_2O_3). Therefore, tourmaline is not suitable as a standard for analyzing boron in silicate glasses, and *vice versa*.

Due to the sharply curved background at the high-energy side of $BK\alpha$, special care should be taken during the background intensity estimation for determining boron content. Using the PeakSight program provided by CAMECA, there is only one option each for linear and exponential regressions, and no further information is available. Figure 4b shows a zoomed-in view of the spectral scan of glass NBS1-0 and a synthetic boron-free rhyolitic glass (RHY-G in Table 1; ref. Zhang *et al.*, 2016). It is revealed by our blank testing on the boron-free glass RHY-G that, for the purpose of estimating on-peak background intensity based on off-peak background intensities at both sides, the results of linear regression and exponential regression using the PeakSight program are slightly higher or lower than the measured “real” background intensity. Our tests also indicate that the linear regression would result in a slightly larger discrepancy value between the “real” and estimated background intensities than the exponential regression. Therefore, we recommend using the exponential regression to estimate on-peak background intensity, although detailed information about the method of exponential regression provided by the PeakSight program is unclear. In addition, we emphasize that, even if the slight discrepancy between the estimated background intensity by exponential regression and the “real” one should be negligible for analyses of high-boron glasses,

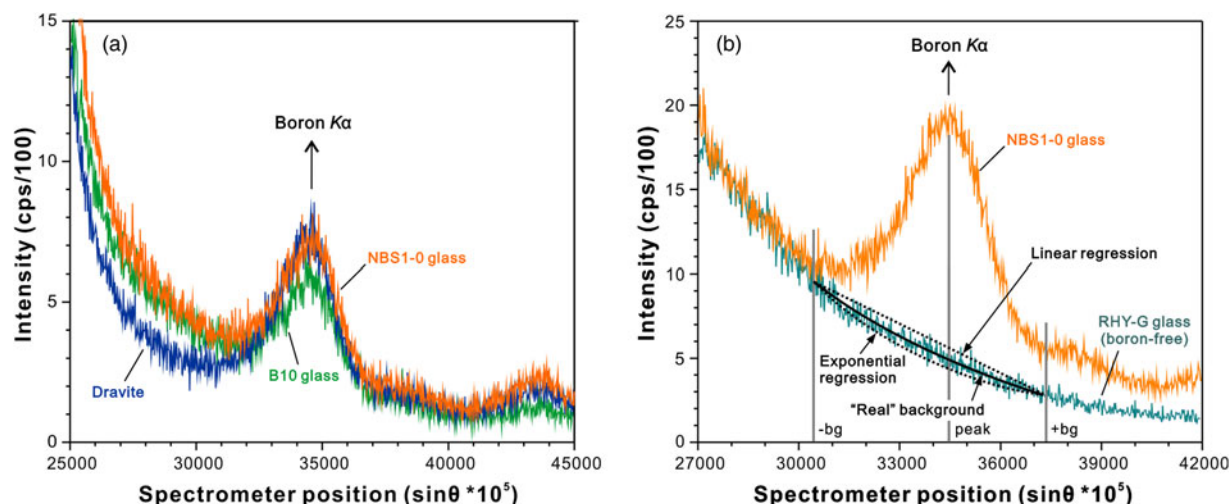


Fig. 4. Characteristics of $BK\alpha$ background. **a:** Comparison between spectral scans of dravite ($B_2O_3 = 10.90$ wt%), sodium borosilicate glass NBS1-0 ($B_2O_3 = 11.32$ wt%) and boron-rich silicate glass B-10 ($B_2O_3 = 9.3$ wt%). It is evident that intensities of $BK\alpha$ signal and background shapes of dravite and NBS1-0 glass are different. Accelerating voltage = 15 keV; beam current = 100 nA. **b:** Background shape of $BK\alpha$ for glasses NBS1-0 and RHY-G (synthetic boron-free rhyolitic glass). The “real” background curve (solid black curve) is between the linear background regression line and the exponential background regression curve (dotted black curves). Accelerating voltage = 5 keV; beam current = 100 nA; dwell time = 100 ms; accumulation number = 3.

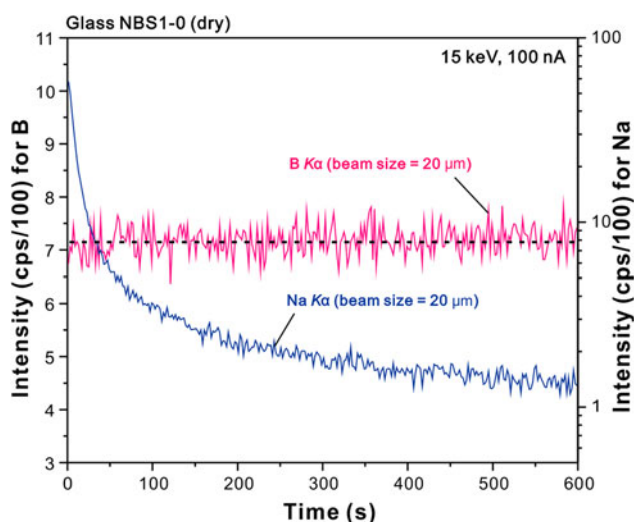


Fig. 5. Record of peak signal intensities for $BK\alpha$ and $NaK\alpha$ in the dry sodium borosilicate glass NBS1-0 as a function of accumulated time using different beam sizes. Accelerating voltage = 5 keV, beam current = 100 nA, beam size = 10 or 20 μ m.

such discrepancy is considered significant for analyses of low-boron contents (e.g., <2 wt%) and must be corrected based on known references. In this study, we use the background determination of the boron-free glass RHY-G as a reference to correct the analyses of other synthetic boron-bearing glasses, because they are similar in major element composition (Table 1).

The dry borosilicate glass NBS1-0 has been well characterized for its composition and homogeneity (Bauer et al., 2017), which allows it to be used as a primary standard for analyzing boron contents in silicic glasses. We tested the potential beam damage of this glass in terms of $BK\alpha$ and $NaK\alpha$ intensities using a beam current of 100 nA. A high beam current is essential for acquiring sufficient intensity for accurate determination of low boron contents. As shown in Figure 5, although the $NaK\alpha$ intensities acquired at the tested conditions (accelerating voltage = 15 keV, beam current = 100 nA, beam size = 10 or 20 μ m) show very strong decreases for a timescale of 600s, the $BK\alpha$ intensities show a systematic consistency if a beam size of 20 μ m was used. Similar intensity variations have been observed if a lower accelerating voltage of 5 or 10 keV is used (diagram not shown). Therefore, it is demonstrated that boron content of the reference glass NBS1-0 can be properly measured with a beam size of

Table 2. Quantification of Spectral Interference from Several Elements on Boron Analysis.

Component	Intensity at $BK\alpha$ peak (cps) from 1 wt% component			Fictive B_2O_3 (wt%) from 1 wt% component		
	15 keV	10 keV	5 keV	15 keV	10 keV	5 keV
B_2O_3 (Glass NBS1-0)	37.5	55.4	95.9	–	–	–
Cl (NaCl)	41.2	42.4	46.0	1.10	0.77	0.48
CaO (An95)	1.15	0.88	0.41	0.031	0.016	0.004
FeO (Fo83)	1.16	1.03	0.51	0.031	0.009	0.005
MnO (Mn_3O_4)	0.39	0.44	0.49	0.010	0.008	0.005

Note: All analyses were done with beam current of 100 nA, beam size of 20 μ m, peak acquisition time of 60 s.

20 μm for primary calibration. We also observed that, for dry silicate glasses (B1, B4, B6, and B10, see Table 1), their $BK\alpha$ intensities also remain systematically constant if a large beam size of 20 μm is used, at the analytical conditions of accelerating voltage of 5–15 keV and beam current of 100 nA (diagram not shown).

We performed calibration for boron on the dry borosilicate glass NBS1-0 using different accelerating voltages of 5, 10, and 15 keV individually. Subsequently, we measured the B_2O_3 contents in several in-house synthetic boron-bearing silicate glasses using the different accelerating voltages. In all calibrations of the reference glass and measurements of samples, the beam current was set as 100 nA, beam size as 20 μm , and peak acquisition time as 60s. The B_2O_3 contents have been corrected, with a linear offline correction approach, for the potential interferences from Ca, Fe, and Mn based on measurements of interference-induced fictive boron signals in plagioclase (An95), olivine (Fo83), and Mn_3O_4 . At the condition of 5 keV, 100 nA and differential mode with window of 4,200 mV, our tests demonstrate that the contributions from spectral interference to the signal of measured $BK\alpha$ intensity are small, with “fictive B_2O_3 ” concentrations from 1 wt% CaO, FeO or MnO (Table 2), much lower than the detection limit of B at specific analytical conditions (Table 1). As a consequence, only high quantities (supposedly >15–20 wt%) of the interfering element CaO, FeO, and even higher quantities of MnO would be really problematic. Because the Cl concentrations in our synthetic glasses are undetectable, i.e., lower than the detection limit (~ 0.02 wt%), the potential spectral interference from Cl on $BK\alpha$ is ignored. In addition, the measured raw B_2O_3 contents by EPMA have been corrected via subtracting the fictive B_2O_3 content of boron-free glass RHY-G, in order to diminish the overestimation of net $BK\alpha$ peak-background intensity using the mode of exponential regression (Fig. 4b).

Testing Result for Beam Damage

We further tested the potential beam damage on a boron-bearing hydrous silicate glass, i.e. glass B0.5 (Table 1). Our testing results (Fig. 6) show that, if a large beam size of 20 μm is used, the $BK\alpha$ intensity is systematically constant for a timescale of 600s, for the tested accelerating voltages from 5 to 15 keV with a high beam current of 100 nA, although a strong decrease in $NaK\alpha$ intensity is evident in all the cases. If a small beam size of 5 μm is used, the $BK\alpha$ intensity shows a rapid increase in the first 150s in the case of using 15 keV and 100 nA. Therefore, it is clear that using a lower accelerating voltage and the defocused beam can not only acquire a high $BK\alpha$ intensity but also efficiently depress the potential beam damage.

Analytical Results of B Concentration in Silicate Glasses

For each analysis, after the major elements other than boron were measured, boron was measured subsequently with a second condition, i.e. accelerating voltages of 5, 10 or 15 keV, beam current of 100 nA, peak acquisition time of 60s. The analytical results are listed in Table 1 and plotted in Figure 7 for comparison with the interpedently measured reference B_2O_3 content in NBS1-I and other synthetic glasses by LA-ICPMS. The good agreement between EPMA and LA-ICPMS data approves the accuracy of EPMA for B_2O_3 content as low as ~ 0.2 wt%. It is notable that, for the high-boron synthetic glasses B4, B6, and B10, the measured B_2O_3 contents from both EPMA and LA-ICPMS are significantly lower than their nominal B_2O_3 contents, i.e. the amount that were added to the starting materials for glass synthesis; this is most likely due to vaporization of boron in the course of

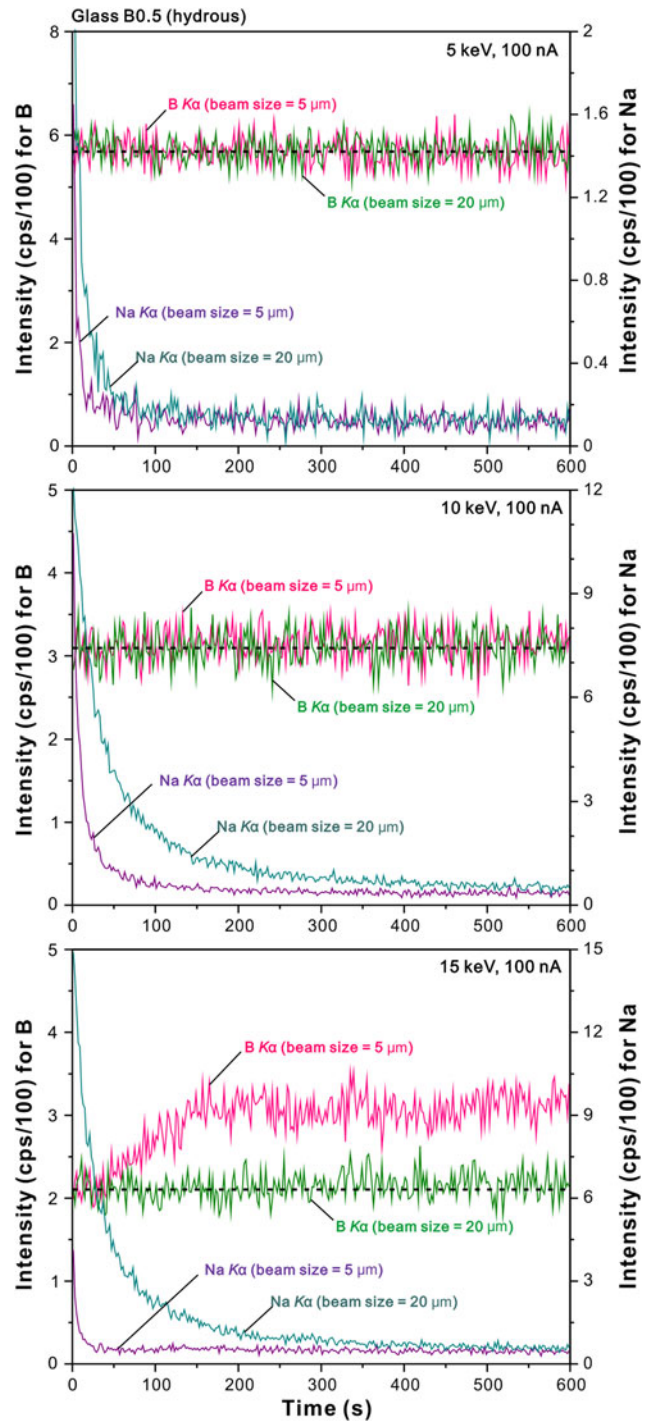


Fig. 6. Record of peak signal for $BK\alpha$ and $NaK\alpha$ in the hydrous glass B0.5 ($B_2O_3 = 0.52$ wt%, $H_2O \approx 4$ wt%) as a function of accumulated time at different analytical conditions. Accelerating voltage = 5, 10 or 15 keV, beam current = 100 nA, beam size = 5 or 20 μm .

glass synthesis in muffle furnace at one atmosphere (e.g., Wenzel & Sanders, 1982; Holtz *et al.*, 1993).

Discussion

Time-Dependent Signal Variation

For analyzing silicate glasses, time-dependent variation in X-ray intensities during electron irradiation, i.e. beam damage, has

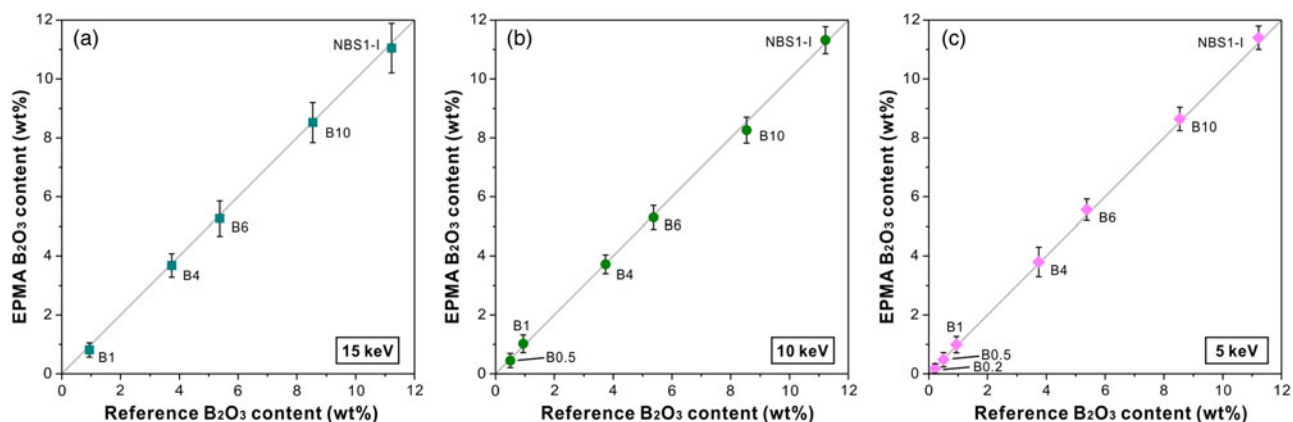


Fig. 7. Comparison of reference B_2O_3 contents versus EPMA data for synthetic glasses using different accelerating voltages (a) 5 keV. (b) 10 keV. (c) 15 keV. Except for NBS1-I glass that its reference B_2O_3 content is after Bauer et al. (2017), other reference B_2O_3 contents of synthetic glasses are measured by LA-ICPMS in this study (see Table 1). Error bar (2σ) for EPMA is shown. Error bar for LA-ICPMS is smaller than symbol size and not shown. The dashed line is 1:1 line.

been found as a serious issue, especially for Na and K which show strong signal loss and for Si and Al which show slight signal gain (Morgan & London, 1996). In addition, such a beam damage is strongly enhanced with increasing H_2O content in the glasses. For measuring boron, our testing for potential beam damage (Figs. 5, 6) shows that the peak $BK\alpha$ intensity remains systematically constant over a long time of electron irradiation (at least 600s) for both dry and hydrous glasses at the analytical conditions of 5–15 keV and 100 nA, if a beam size of $20\mu m$ is used. In this study, in order to minimize the beam damage, major elements other than boron were first measured with a low beam current of 5 nA with a total acquisition time of 40s; consequently, it is expected that the electron irradiation during this stage should have little damage effect on the boron signal measured afterward. Our testing also shows that, for the hydrous boron-bearing glass B0.5, if a small beam size of $5\mu m$ is used for the analytical condition of 15 keV and 100 nA, the detected peak $BK\alpha$ intensity exhibits a strong increase in the first 150s (Fig. 6). This is interpreted as, at this analytical condition, the glass matrix has been “adequately” damaged by electron irradiation to result in either migration of boron or changes in absorption for $BK\alpha$ X-ray. Nevertheless, at other tested analytical conditions, it seems that potential beam damage affecting boron analysis is minimal.

Detection Limit and Uncertainty

In principle, the detection limit refers to the lowest concentration that can be distinguished by measuring the spectral peak above statistical background fluctuations, and its value is recommended to be that corresponding to a peak count higher than the mean background count by three times the standard deviation of the background count (Analytical Methods Committee, 1987). Practically, for the analytical protocol used in this study, we can obtain the detection limits for different analytical conditions as three times the standard deviations of the B_2O_3 contents measured for the boron-free glass RHY-G. Correspondingly, we obtain B_2O_3 detection limits as 0.18, 0.27, and 0.63 wt% while using an accelerating voltage of 5, 10, and 15 keV, respectively (Table 1). Uncertainty in the measurements is partly dependent on the compositional similarity between the boron-free glass and the unknown samples, and the resultant maximum uncertainty equals to its fictive B_2O_3 content that is within ca. 0.2–0.4 wt% (Table 1).

Improving EPMA of Boron

Analysis of boron concentration in tourmalines, borides and some boron-rich glasses has been tested in previous studies (McGee et al., 1991; Bastin & Heijligers, 1992,2000; McGee & Anovitz, 1996; Fournelle et al., 2000; Meier et al., 2011). However, analysis of low boron concentrations in silicate glasses, as well as other light elements, is a significant challenge due to a number of issues, such as low efficiency of X-ray excitation, highly curved background, and potential spectral interferences from other elements (Fialin et al., 1996; McGee & Anovitz, 1996; Morgan, 2015; see also statements in Introduction).


This study demonstrates that the internal interferences from the Mo- B_4C LMS crystal (McGee & Anovitz, 1996) can be eliminated via an optimized differential mode of PHA, but the high-energy side background of $BK\alpha$ in boron-bearing silicate glasses (Fialin et al., 1996) is still strongly high and cannot be effectively reduced. Quantitative calibration of the potential spectral interferences (e.g., Ca, Fe, and Mn) on $BK\alpha$ should be performed for accurate analyses of low boron concentrations. In addition, for simulating this strongly curved background shape, an exponential regression provides a better estimation of on-peak background intensity based on measured off-peak background intensities. For analyzing low boron concentrations, it is important to perform correction for the discrepancy between the “real” on-peak background and estimated background from off-peak measurements, ideally using a boron-free glass with similar major element composition to unknown samples.

However, in many cases, it is expected that a useful boron-free glass for simulating the background shapes of unknown glasses may be unavailable. Therefore, for a more routine procedure to obtain a high analytical accuracy for low boron concentrations in silicate glass, more accurate modeling of the background curve is demanded, which requires intensity measurements on multi-point background positions. Similar approaches have been discussed and applied on analyses of other trace elements by EPMA (e.g., Donovan et al., 2011; Allaz et al., 2019), and such a function has been implemented in the Probe Software for EPMA of Donovan (<http://probesoftware.com/>). It is expected that, if the Probe Software is applied, due to the useful function that background estimate can be analyzed, verified, or modified after the performance of analysis, accurate analyses of low boron concentrations in silicate glasses would be more easily achievable. However, without access to this software, the protocol

used in this study provides an alternative way to accurately measure low boron concentrations (≥ 0.2 wt% B_2O_3) in silicate glasses.

Conclusions

Using a large d -spacing diffraction crystal (Mo- B_4C LMS crystal, PC3 or LDE3), we were able to accurately analyze boron content in silicate glasses for a wide range of B_2O_3 content, i.e. from ~ 0.2 wt% to over 10 wt%. For analyzing low boron contents in silicate glasses, the optimized analytical setting involves a differential mode of PHA, a low accelerating voltage, exponential regression for on-peak background, careful calibration of potential spectral interferences from other elements, and an appropriate boron-rich silicate glass standard.

Author ORCID.  Chao Zhang, 0000-0001-7019-5075; Renat R. Almeev, 0000-0003-0652-9469

Acknowledgments. We thank Harald Behrens (LUH) for providing borosilicate glasses NBS1-0 and NBS1-I, and Michael Wiedenbeck (GFZ at Potsdam) for providing referencedravitte. Ingo Horn (LUH) is appreciated for his assistance of LA-ICPMS analysis. The stay of Lining Cheng at the Institute of Mineralogy, Leibniz University Hannover, was funded by China Scholarship Council (CSC). We thank Julien M. Allaz, another anonymous reviewer and Editor Daniel Ruscitto for their critical and insightful comments that have greatly improved this paper. Requests for boron-bearing glasses used in this study as microanalytical references can be addressed to the corresponding author. This study was supported partly by Deutsche Forschungsgemeinschaft (DFG) project BE 1720/40.

References

- Allaz JM, Williams ML, Jercinovic MJ, Goemann K & Donovan J (2019). Multipoint background analysis: Gaining precision and accuracy in microprobe trace element analysis. *Microsc Microanal* **25**(1), 30–46.
- Analytical Methods Committee (1987). Recommendations for the definition, estimation and use of the detection limit. *Analyst* **112**(2), 199–204.
- Bastin G & Heijligers H (1992). Present and future of light element analysis with electron beam instruments. *Microbeam Anal* **1**(2), 61–73.
- Bastin GF & Heijligers HJM (2000). Quantitative electron probe microanalysis of boron. *J Solid State Chem* **154**(1), 177–187.
- Bauer U, Behrens H, Reinsch S, Morin E & Stebbins J (2017). Structural investigation of hydrous sodium borosilicate glasses. *J Non-Cryst Solids* **465**, 39–48.
- Berndt J, Liebske C, Holtz F, Freise M, Nowak M, Ziegenbein D, Hurkuck W & Koepke J (2002). A combined rapid-quench and H₂-membrane setup for internally heated pressure vessels: Description and application for water solubility in basaltic melts. *Am Mineral* **87**(11–12), 1717–1726.
- Demers H, Horny P, Gauvin R & Lifshin E (2002). WinX-Ray: A new monte-carlo program for the simulation of X-ray and charging materials. *Microsc Microanal* **8**(S02), 1498–1499.
- Dingwell DB, Pichavant M & Holtz F (1996). Experimental studies of boron in granitic melts. *Rev Mineral Geochem* **33**(1), 330–385.
- Donovan JJ, Lowers HA & Rusk BG (2011). Improved electron probe microanalysis of trace elements in quartz. *Am Mineral* **96**(2–3), 274–282.
- Dyar MD, Wiedenbeck M, Robertson D, Cross LR, Delaney JS, Ferguson K, Francis CA, Grew ES, Guidotti CV & Hervig RL (2001). Reference minerals for the microanalysis of light elements. *Geostand Newslett* **25**(2–3), 441–463.
- Fialin M, Rémy H, André JM, Chauvineau JP, Rousseaux F, Ravet MF, Decanini D & Cambriel E (1996). Extending the possibilities of soft X-ray spectrometry through the etching of layered synthetic microstructure monochromators. *X-Ray Spectrom* **25**(2), 60–65.
- Fournelle J, Donovan J, Kim S & Perepezkov J (2000). Analysis of boron by EPMA: Correction for dual Mo and Si interferences for phases in the Mo-B-Si system, Institute of Physics Conference Series, London, pp. 425–426.
- Guillong M, Meier DL, Allan MM, Heinrich CA & Yardley BW (2008). Appendix A6: SILLS: A MATLAB-based program for the reduction of laser ablation ICP-MS data of homogeneous materials and inclusions. *Mineral Assoc Canada Short Course* **40**, 328–333.
- Holtz F, Dingwell DB & Behrens H (1993). Effects of F, B_2O_3 and P_2O_5 on the solubility of water in haplogranite melts compared to natural silicate melts. *Contrib Mineral Petrol* **113**(4), 492–501.
- Horn I, von Blanckenburg F, Schoenberg R, Steinhöfel G & Markl G (2006). *In situ* iron isotope ratio determination using UV-femtosecond laser ablation with application to hydrothermal ore formation processes. *Geochim Cosmochim Acta* **70**(14), 3677–3688.
- Jochum KP, Dingwell DB, Rocholl A, Stoll B, Hofmann AW, Becker S, Bismehn A, Bessette D, Dietze H-J, Dulski P, Erzinger J, Hellebrand E, Hoppe P, Horn I, Janssens K, Jenner GA, Klein M, McDonough WF, Maetz M, Mezger K, Mürker C, Nikogosian IK, Pickhardt C, Raczek I, Rhede D, Seufert HM, Simakin SG, Sobolev AV, Spettel B, Straub S, Vincze L, Wallianos A, Weckwerth G, Weyer S, Wolf D & Zimmer M (2000). The preparation and preliminary characterisation of eight geological MPI-DING reference glasses for in-situ microanalysis. *Geostand Newslett* **24**(1), 87–133.
- Jochum KP, Weis U, Stoll B, Kuzmin D, Yang Q, Raczek I, Jacob DE, Stracke A, Birbaum K, Frick DA, Günther D & Enzweiler J (2011). Determination of reference values for NIST SRM 610–617 glasses following ISO guidelines. *Geostand Geoanal Res* **35**(4), 397–429.
- Kobayashi H, Toda K, Kohno H, Arai T & Wilson R (1995). The study of some peculiar phenomena in ultra-soft X-ray measurements using synthetic multilayer crystals. *Adv X-Ray Anal* **38**, 307–312.
- London D (1987). Internal differentiation of rare-element pegmatites: Effects of boron, phosphorus, and fluorine. *Geochim Cosmochim Acta* **51**(3), 403–420.
- London D, Morgan GB & Wolf MB (1996). Boron in granitic rocks and their contact aureoles. *Rev Mineral Geochem* **33**(1), 299–330.
- McGee JJ & Anovitz LM (1996). Electron probe microanalysis of geologic materials for boron. *Rev Mineral* **33**, 770–788.
- McGee JJ, Slack JF & Herrington CR (1991). Boron analysis by electron microprobe using MoB₄C layered synthetic crystals. *Am Mineral* **76**, 681–684.
- Meier DC, Davis JM & Vicenzi EP (2011). An examination of kernite (Na₂B₄O₆(OH)₂·3H₂O) using X-ray and electron spectroscopies: Quantitative microanalysis of a hydrated low-Z mineral. *Microsc Microanal* **17**(5), 718–727.
- Morgan VI GB (2015). Practical aspects of the electron probe analysis of boron in silicates using a LSM device with large 2d. *Microsc Microanal* **21**, 1141.
- Morgan VI GB & London D (1996). Optimizing the electron microprobe analysis of hydrous alkali aluminosilicate glasses. *Am Mineral* **81**, 1176–1185.
- Pichavant M (1981). An experimental study of the effect of boron on a water saturated haplogranite at 1 Kbar vapour pressure. *Contrib Mineral Petrol* **76**(4), 430–439.
- Schmidt BC (2004). Effect of boron on the water speciation in (aluminosilicate) melts and glasses. *Geochim Cosmochim Acta* **68**(24), 5013–5025.
- Tiepolo M, Zanetti A & Vannucci R (2005). Determination of lithium, beryllium and boron at trace levels by laser ablation-inductively coupled plasma-sector field mass spectrometry. *Geostand Geoanal Res* **29**(2), 211–224.
- Wenzel JT & Sanders DM (1982). Sodium and boron vaporisation from a boric oxide and a borosilicate glass melt. *Phys Chem Glasses* **23**(2), 47–52.
- Zhang C, Koepke J, Albrecht M, Horn I & Holtz F (2017). Apatite in the dike-gabbro transition zone of mid-ocean ridge: Evidence for brine assimilation by axial melt lens. *Am Mineral* **102**(3), 558–570.
- Zhang C, Koepke J, Wang L-X, Wolff PE, Wilke S, Stechern A, Almeev R & Holtz F (2016). A practical method for accurate measurement of trace level fluorine in Mg- and Fe-bearing minerals and glasses using electron probe microanalysis. *Geostand Geoanal Res* **40**(3), 351–363.